Clinical Imaging 55 (2019) 53–64

Contents lists available at ScienceDirect

Clinical Imaging

journal homepage: www.elsevier.com/locate/clinimag

Cardiothoracic Imaging

Interatrial septum: A pictorial review of congenital and acquired pathologies and their management☆,☆☆,☆☆☆,☆☆☆☆

Pegah Khoshpouri[a], Parisa Khoshpouri[b], Arash Bedayat[c], Kianoush Ansari-Gilani[d], Hamid Chalian[e,*]

[a] Russell H. Morgan Department of Radiology and Radiological Sciences, Johns Hopkins University School of Medicine, Baltimore, MD, USA
[b] Department of Emergency Radiology, University of British Columbia, Vancouver, British Columbia, Canada
[c] Department of Radiological Sciences, University of California-Los Angeles, Los Angeles, California, USA
[d] Department of Radiology, University Hospitals Cleveland Medical Center, Cleveland, OH, USA
[e] Department of Radiology, Duke University Medical Center, Durham, NC, USA

ARTICLE INFO

Keywords:
Atrial septum
Congenital
Acquired
Magnetic resonance imaging
Computed tomography

ABSTRACT

There are many different congenital abnormalities and acquired pathologies involving the interatrial septum. Differentiation of these pathologies significantly affects patient management. We have reviewed the various interatrial septal pathologies and discussed their congenital associates, clinical significance, and management. After reading this article, the reader should be able to better characterize the interatrial septal pathologies using the optimal imaging tools, and have a better understanding of their clinical significance and management.

1. Introduction

Diagnosis of interatrial septal pathology is often challenging because the clinical presentations of these diseases are often nonspecific, and accurate diagnosis from common imaging modalities, like echocardiography, can suffer from technical limitations. Some congenital abnormalities of the interatrial septum are associated with a wide spectrum of other abnormalities. Understanding and detecting these associated abnormalities can affect patient management.

Recent advances in cardiac magnetic resonance imaging (MRI) and computed tomography (CT) have made it possible for earlier diagnosis and better characterization of pathologies involving the interatrial septum [1,2]. Radiologists play an important role in the management of interatrial lesions, as some of the diagnoses are found incidentally, especially in the adult population. Accurate interpretation of these diagnoses can have a profound effect on patient outcome.

The purpose of this article is to review the congenital and acquired diseases involving the interatrial septum, including their clinical significance and associated findings. We hope to familiarize radiologists with the best imaging modalities and sequences for detection and differentiation of these pathologies, and review appropriate clinical management. We have included different cases and imaging techniques to better illustrate the radiologic features of interatrial septal pathologies.

2. Congenital abnormalities of the interatrial septum

2.1. Atrial septal defects (ASDs)

ASDs are the second most common congenital heart defects, after ventricular septal defects, accounting for approximately 10% of all congenital heart diseases. Since many ventricular septal defects are small and close spontaneously, ASDs are the most common congenital heart defects to become symptomatic in adulthood.

In general, a pulmonary to systemic flow ratio (Qp:Qs) $>$ 1.5:1 is a widely accepted indication for surgery in stable ASD patients with no contraindications. Patients with Qp:Qs $<$ 1.5:1 will undergo closure in the setting of paradoxical embolization or right heart volume overload.

☆ The authors confirm that this work is original and has not been published elsewhere nor is it currently under consideration for publication elsewhere, in whole or in part. All the authors have approved to submit this manuscript to Cardiovascular Diagnosis and Therapy.
☆☆ There is no conflict of interest or industry support for this manuscript.
☆☆☆ This is a pictorial review and exempted from IRB.
☆☆☆☆ This research did not receive any specific grant from funding agencies in the public, commercial, or not-for-profit sectors.
* Corresponding author at: Department of Radiology, Duke University Medical Center, 2301 Erwin Rd, Durham, NC 27705, USA.
E-mail address: Hamid.chalian@duke.edu (H. Chalian).

https://doi.org/10.1016/j.clinimag.2019.02.002
Received 17 October 2018; Received in revised form 28 January 2019; Accepted 5 February 2019

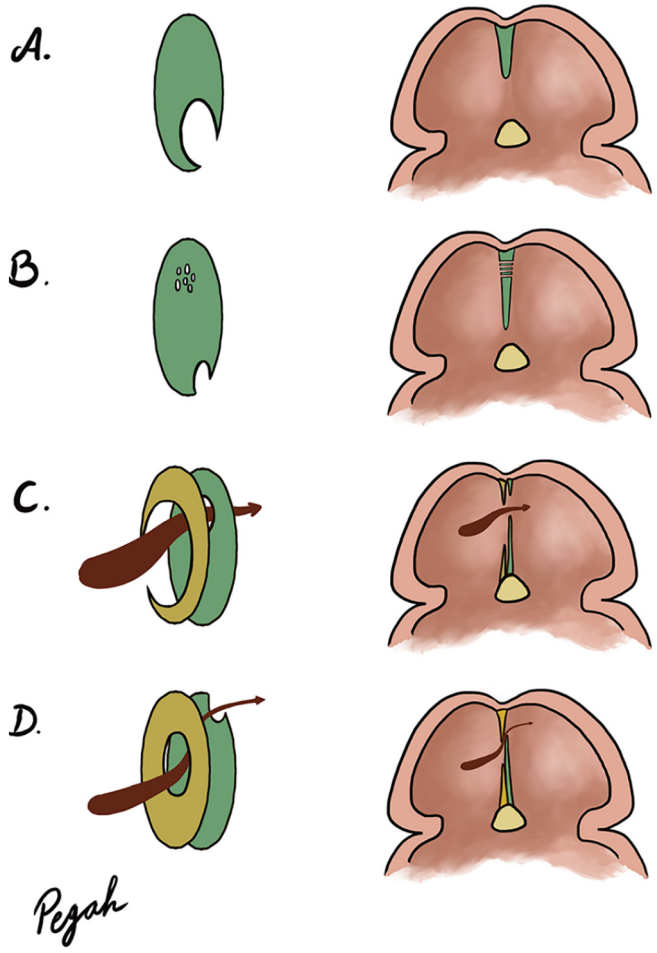

Fig. 1. In utero development of the interatrial septum. A crest of tissue (septum primum, green septum) grows from the roof of the atria (A). Several small fenestrations develop at the superior aspect of the septum primum and eventually coalesce to form ostium secundum (B). An infolding of the atrial walls to the right of the septum primum develops and makes the septum secundum (yellow septum). A hole remains more inferiorly in septum secundum which with ostium secundum allow right to left shunting of oxygenated blood from the umbilical arteries. Eventually, septum secundum covers ostium secundum. Ostium primum will cover the hole in septum secundum (fossa ovalis) (C). Eventually the two septa fuse together except at the anterosuperior edge of the fossa ovalis. This tunnel/flap valve allows necessary fetal right to left shunt (D). (For interpretation of the references to color in this figure legend, the reader is referred to the web version of this article.)

There are five major types of ASDs based on the location of defect in the septum which will be discussed below.

2.1.1. Patent foramen ovale (PFO)

The atrial septa primum and secundum flaps fuse to form the fossa ovalis. When there is incomplete fusion of these flaps, the foramen ovale remains patent. This incomplete fusion leaves a channel-like communication between the right and left atria. When there is a shunt through this communication, it is called a PFO. Please refer to Fig. 1 for better understanding of the embryogenesis of the interatrial septum. The incidence of PFO is as high as 34% during the first three decades of life and declines with age [3,4]. Most cases of PFO are small and remain asymptomatic; however, PFOs have been associated with transient ischemic attack and stroke due to the potential of a venous thrombus to pass from the right atrium into the systemic circulation via the PFO. The annual incidence of transient ischemic attack and cerebral stroke in patients with PFO is about 3.5% [5].

EKG-gated cardiac CT and MRI can help identify a PFO. To confirm the presence of a PFO, a channel-like tunnel in the interatrial septum or a flap valve on the left atrial side of the foramen should be visualized in addition to either communication of contrast on CT [6,7] or dephasing signal on MRI to confirm patency (Fig. 2). Presence of a channel-like tunnel along the interatrial septum alone is not sufficient to make the diagnosis of PFO since it can be a normal variant of the fossa ovalis. Saremi et al. showed that multidetector EKG-gated CT provides detailed information on the morphologic features of PFO including the length and diameter of the opening of the PFO tunnel, presence of septal aneurysm, and PFO shunt. They graded PFO shunt on EKG-gated CT based on the length of contrast agent jet. They reported more left to right shunt in patients with shorter PFO tunnel length and those with septal aneurysm. [8].

Anatomic variations of the interatrial septum can mimic PFO. Septal pouch is a recently described anatomic entity within the interatrial septum. This entity was first described in an autopsy study by Krishnan and Salazar [9]. A septal pouch is a diverticulum–like structure on the left or right side of the interatrial septum that occurs when the septum primum and septum secundum are partially fused but the PFO channel is absent. Septal pouch is more common on the left side of the interatrial septum [10]. Care must be taken not to confuse PFO with septal pouch on CT or MRI interpretation. Presence of shunt through the interatrial septum, or visualization of a patent PFO channel are in favor of PFO.

Isolated PFO does not require any medical or surgical intervention. Currently, no consensus exists in treatment of patients with PFO and transient ischemic attack or stroke. Available treatment options include 1) Medical treatment (antiplatelet/anticoagulant), 2) Percutaneous closure device placement, and 3) Surgical closure. Several case series has shown high recurrence rate (4% to 20% per year) of TIA/stroke in PFO patients undergoing medical treatment [11]. There is a growing clinical interest in the use of anticoagulant medications like warfarin over antiplatelet medication, despite increased risk of hemorrhage. However, contradicting data has been published from post hoc analysis of the from post hoc analyses of the Warfarin-Aspirin Recurrent Stroke Study (WARSS) trial showing no difference in occurrence of the ischemic neurologic events or death between aspirin and warfarin groups, although warfarin was shown to be associated with one-third fewer recurrent strokes than aspirin [12]. Decision on used of antiplatelet or anticoagulation treatment need to be made based on individual factors [13]. There are 5–7 different closure devises available to be used for percutaneous closure of the PFO in patients with TIA/stroke. Although none of these devices has FDDA pre-market approval for PFO closure, the Amplatzer PFO Occluder and CardioSEAL may be used under Food and Drug Administration mandated humanitarian device exemption (HDE) guidelines [11]. Annual recurrence rate for TIA/stroke post percutaneous closure has been < 4% [14]. Although supporting data is limited due to single institutional nature or selective enrolment, surgical closure of PFO in patients with TIA/stroke appears a safe and effective treatment option [15].

2.1.2. Ostium secundum ASD

The ostium secundum ASD is the most common type making up 70% of all ASDs. Unlike other types of ASD, ostium secundum ASD has a female predilection (65%–75%). In ostium secundum ASD, the defect is in the midseptal region. Embryologically, the ostium secundum ASD is caused by excessive resorption of the septum primum or deficient growth of the septum secundum (Fig. 1). Most cases of ostium secundum ASD are found in isolation. MRI has excellent tissue characterization and is a good modality to show the defect in the midportion of the interatrial septum. Additional critical information, such as the presence of a shunt across the defect and assessment of cardiac function, can be obtained by cardiac MRI (Fig. 3). Using velocity-encoded sequence, flow across the ASD can be measured either directly by imaging the ASD en face, or indirectly by velocity-encoded imaging of the pulmonary artery and aorta [16]. Although one of these techniques

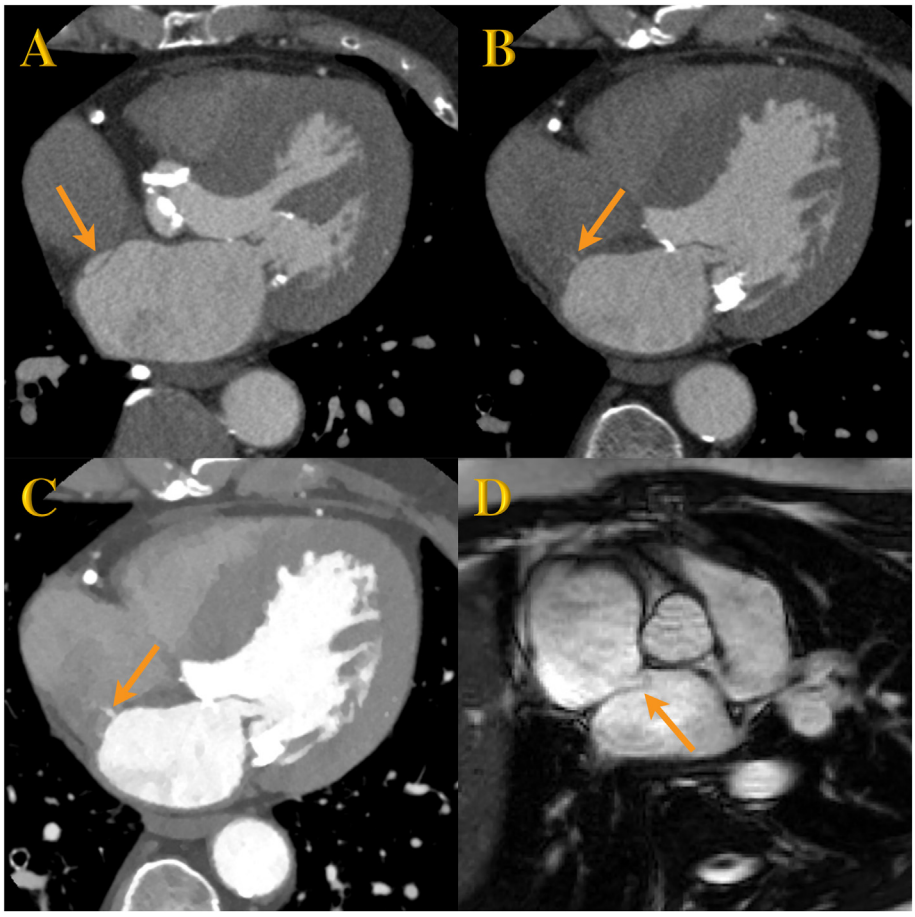

Fig. 2. Spectral EKG-gated cardiac CT of a 79-year-old man with severe aortic stenosis shows a channel-like appearance of the interatrial septum (arrow in A), suggestive of a patent foramen oval (PFO). The contrast agent jets from left atrium to the right atrium (arrow in B) confirm abnormal communication as well as a PFO. The jet is more conspicuous in the 40 keV monoenergetic image (arrow in C). Bright blood sequence demonstrates either a PFO taking a tunneled intra-septal course or a flap valve on the left atrial side of the foramen ovale (arrow in D).

are usually favored in different institutions, experts believe that ASD flow measurement by direct en face technique is more accurate and better correlates with invasive oximetry [16]. A four step approach can be used to obtain the optimal true en face view. Step 1, Use the cine SSFP images to identify the 4 chamber and biatrial views in which flow across the septum or fossa ovalis can be visualized. Step 2, Obtain a through-plane velocity encoding MR image. Set low velocity encoding in this phase (~60 cm/s) to have good sensitivity. This will provide an approximate en face view of the ASD flow. Step 3, make an in-plane velocity encoding view in 4 chamber and biatrial orientations centered through the defect/flow seen in step 2. Step 4, Use the 2 orthogonal images from step 3 and obtain a final through-plane velocity encoding MR image. This will make the true en face velocity encoding image [16].

Precise localization of the atrial septal defect is critical for differentiation of different types of atrial septal defects. If the defect is not localized accurately, ostium secundum ASD might be mistaken with sinus venosus ASD or even ostium primum ASD. Accurate localization of the atrial septal defect could be done with high quality echocardiography, gated CT or MRI [6]. To avoid localization mistakes and provide information for interventionalists and surgeons regarding the exact location of the ASD and amount of septal tissue available around the defect, it is useful to obtain or reconstruct 4 chamber view on gated CT and MRI. Stack Cine images in 4 chamber and short axis view covering the atria is also helpful. Obtaining true en face view through the interatrial defect on cardiac MRI (as detailed above) can provide accurate

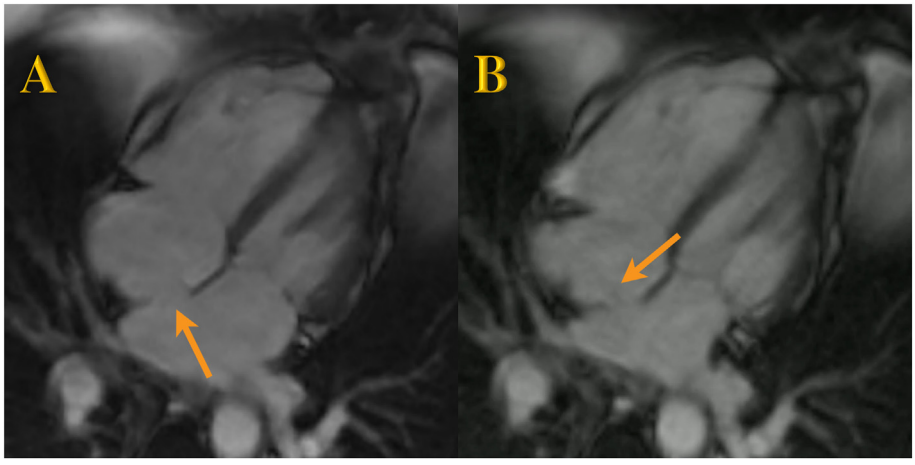

Fig. 3. Four-chamber view bright blood sequence demonstrates a defect in the mid portion of the atrial septum (arrow in A) consistent with ostium secundum ASD. Single shot of steady-state free precession (SSFP) cine shows faint dephasing signal across the ASD to the right atrium suggestive of a mild left to right shunt (arrow in B).

information about the size and location of the defect, and available septal tissue adjacent to ASD.

Different correction strategies and options make differentiation of atrial septal defects more important. Closure should be considered in all hemodynamically significant ostium secundum ASDs, regardless of patients' age or symptoms. Unlike other types of ASD, for which surgical correction is the standard of care, percutaneous closure devices have been developed over the last decade for treatment of ostium secundum ASDs. The Amplatzer Septal Occluder (ASO) and Helex closure device are approved by the FDA in the United States. However, surgical correction of an ostium secundum ASD remains a viable option in many developing countries [17]. The advantage of percutaneous closure over traditional surgery is a shorter hospital stay and lower complication rate while maintaining a similar success rate of closure [18,19].

2.1.3. Ostium Primum ASD

In ostium primum ASD, the defect is close to the atrioventricular valves. Since this type of ASD can be associated with an atrioventricular septal defect, it also falls within the spectrum of the atrioventricular (AV) septal defects, also known as endocardial cushion defects or AV canal defects. The complete form of this defect includes a single large AV valve with a large ASD and ventricular septal defect [20,21].

Cardiac MRI is the imaging modality of choice for assessment of ostium primum ASDs since critical information on the extension and hemodynamic significance of the defect, as well as other possible cardiac anomalies can be obtained (Fig. 4). EKG-gated CT can also demonstrate ostium primum ASD and associated cardiac anomalies in detail [6,22]. One of the major advantages of cardiac MRI over CT is lack of radiation. Since ostium primum cases need to be surgically managed in early childhood, radiation is a real concern. Cardiac MRI can provide information on the extent of the endocardial cushion defect and assess shunt through the interatrial defect. Disadvantage of cardiac MRI would be the length of study and necessity of general anesthesia in children. General anesthesia is less frequently required for cardiac CT imaging of children. Despite radiation exposure, Cardiac CT assessment of the complex congenital heart diseases is increasingly popular. Cardiac CT allows assessment of the extracardiac anatomy in addition to the intracardiac anatomy and defects. However, cardiac MRI is superior for assessment of flow quantification and intracardiac anatomy when compared to cardiac CT. Some specific anatomic details such as coronary artery origin are better seen using cardiac CT than cardiac MRI [23].

Currently, surgical repair is the standard of choice for patients with ostium primum ASD due to inadequate septal rims to secure device deployment, and proximity to the defect to the AV valves.

2.1.4. Sinus venosus ASD

The defect in this type of ASD is most commonly situated in the right atrium near the entrance of the superior vena cava (SVC), and is less likely located near the entrance of the inferior vena cava (IVC). This type of ASD is uncommon and is associated with other cardiac anomalies including partial anomalous pulmonary venous drainage (usually drainage of the right upper lobe pulmonary vein into the SVC or right atrium) [20].

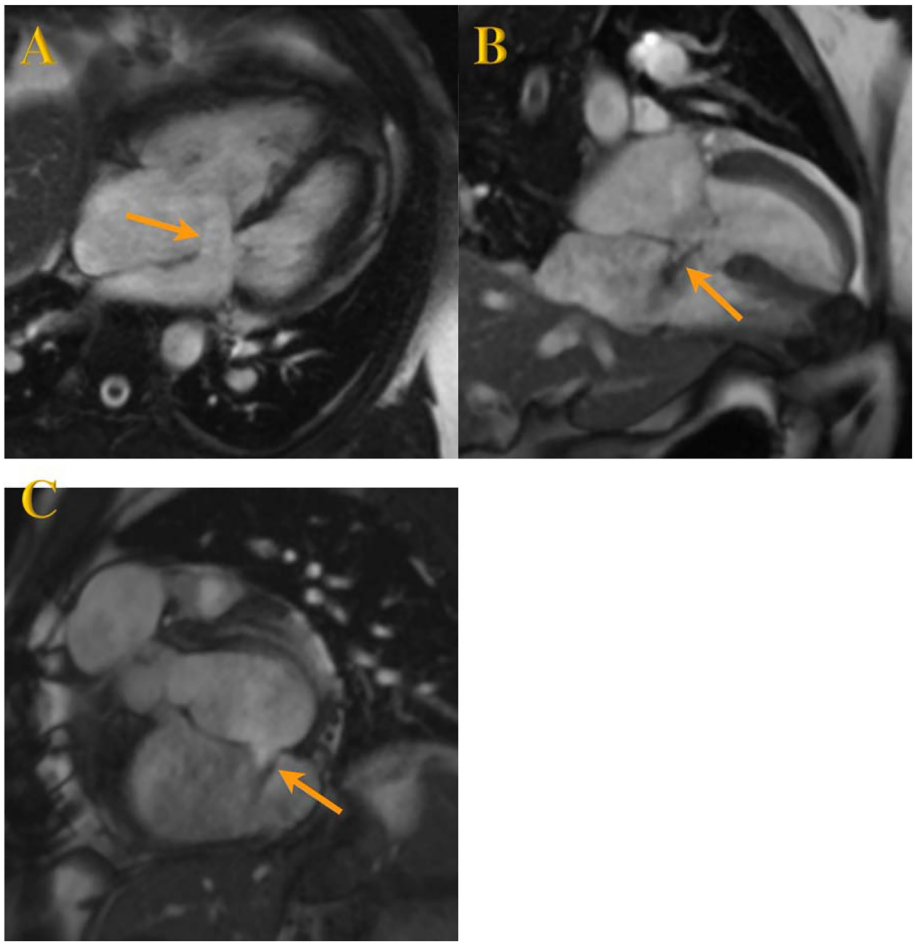

Fig. 4. A 60-year-old male with history of atrioventricular canal repair in childhood presented with atrial fibrillation. There is a residual defect measuring 2.7 × 2.0 cm at the inferior aspect of the base of the interatrial septum consistent with an ostium primum atrial septal defect (image A). On steady-state free precession (SSFP), a dephasing jet demonstrates left to right shunting (image B and C). The direct flow across the defect measured 5.9 L/min with Qp/Qs of 2.4.

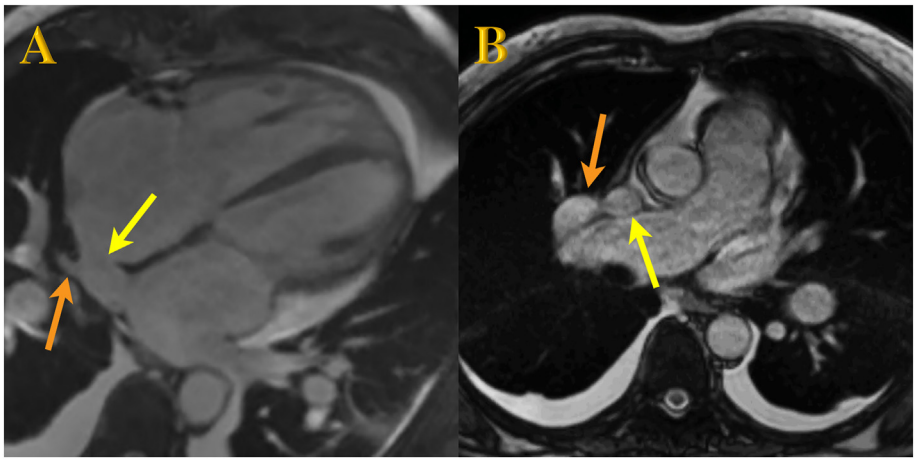

Fig. 5. Sinus venosus ASD (yellow arrow in A). The right middle lobe pulmonary vein (orange arrow in A) drains into the septal defect and the right upper lobe pulmonary vein (orange arrow in B) drains into the SVC (yellow arrow in B), consistent with partial anomalous pulmonary venous return. Qp/Qs measured 5.6 representing a significant shunt. (For interpretation of the references to color in this figure legend, the reader is referred to the web version of this article.)

EKG-gated CT and cardiac MRI (Fig. 5) can show the defect and other associated cardiovascular anomalies. As in cases of ostium primum ASD, lack of adequate septal rims to secure device deployment, and proximity to the vena cava makes surgical repair a more standard treatment for sinus venosus ASDs.

2.1.5. Coronary sinus ASD (unroofed coronary sinus)

An unroofed coronary sinus is the rarest type of ASD. In this form of ASD, part or all of the walls between the coronary sinus and left atrium is absent. This defect can be in the form of small fenestrations to a large defect. There is a high association between an unroofed coronary sinus and a persistent left superior vena cava (Fig. 6) as well as other congenital anomalies of the heart including heterotaxia syndrome [24]. Clinical presentation of an unroofed coronary sinus is nonspecific and dependent on the degree of left-to-right shunt and the size of the defect which contributes to the patients' risk for stroke and brain abscess [25].

Precise assessment of all associated cardiovascular abnormalities and the degree of shunting are essential for treatment planning [26]. Kwak, et al. reported a case of unroofed coronary sinus with total anomalous pulmonary venous return mimicking core triatriatum in the left atrium. Authors found 3D imaging from CT scan helpful for diagnosis and preoperative planning [27]. A high quality gated cardiac CT with 3D rendering can be extremely helpful in understanding the anatomy and associated cardiac anomalies.

Treatment of the unroofed coronary sinus consists of surgical rerouting of the coronary sinus to the right atrium. In cases with associated persistent left superior vena cava, rerouting of the persistent left superior vena cava to the right atrium is also required [28].

2.2. Atrial septal aneurysm (ASA)

ASA is a congenital anomaly characterized by focal bulging of the interatrial septum into the right and/or left atrium during the cardiac cycle. Although ASA can be an isolated finding, there is a strong association of ASA with a patent foramen ovale which places these patients at risk for cryptogenic stroke. A 33-fold higher risk of stroke has been reported in patients with a combination of ASA and patent foramen ovale [29,30]. Perforation of the ASA can place the patient at increased risk for paradoxical embolism [31]. Association of ASA with mitral valve prolapse and supraventricular tachyarrhythmias has also been reported in the literature [32,33].

Hanley established diagnostic criteria for ASA which includes protrusion of the interatrial septum by at least 1.5 cm beyond the plane of the atrial septum or at least 1.5 cm excursion of the interatrial septum during the cardiac cycle in total amplitude with a basal diameter of the aneurysm of at least 1.5 cm [34]. According to Hanley's diagnostic criteria that modified by Pearson, four types of ASA can be determined morphologically: 1) Type 1A, constant protrusion of the ASA toward the right atrium. 2) Type 1B, predominant protrusion to the right atrium with small systolic movement toward left. 3) Type 1C, protrusion toward the left atrium with Valsalva maneuver. 4) Type 2C, constant protrusion toward the left atrium [34,35]. Transesophageal echocardiography (TEE) is significantly more sensitive in the detection of ASA compared to transthoracic echocardiography (TTE). Diagnosis of ASA can be challenging using echocardiography. ASA can mimic core triatriatum sinister or atrial mass on echocardiography [30,36]. MRI is the imaging study of choice for suspicious cases when echocardiography is equivocal. An ASA can be well evaluated on steady-state free precession (SSFP) cine MRI sequence (Fig. 7). MRI can also show a signal void through the ASA representing shunt if a patent foramen ovale is present.

Available studies have shown that risk of recurrent stroke is not high enough to warrant long term anticoagulation therapy or surgical intervention. Antiplatelet treatment (aspirin) is an effective treatment for incidental ASA [37].

3. Acquired pathologies involving interatrial septum

3.1. Interatrial septal lipoma

Lipoma is the second most common primary benign cardiac tumor making up approximately 10% of all primary cardiac tumors [38]. The two most common adipose-containing lesions of the heart are lipoma and lipomatous hypertrophy of the interatrial septum (LHIS). Unlike LHIS, lipomas are generally well-encapsulated and contain well differentiated mature fat cells [1]. It can occur in any location in the heart, including the sub-endocardial layer, which accounts for half of all cases, and either sub-epicardial or mid-myocardial layers, which account for the other half [1,38]. Lipoma usually occurs in younger age groups compared to LHIS [1]. Multifocal lipomas may be seen in patients with tuberous sclerosis. Lipomas grow slowly and since the location of the tumor differs in each case, patients may present with various manifestations [38,39]. Patients with a cardiac lipoma are usually asymptomatic until the lesions become large enough to exert some clinically significant mass effect. The size and location of a cardiac lipoma contributes to the potential symptoms such as dyspnea, chest pain (due to compression effect on coronary arteries), dizziness and syncope (due to outflow obstruction), and arrhythmias (due to compression of nerve conducting tissues) [1,38,39].

Echocardiography can detect a mass lesion and identify its location; however, this modality is limited in its ability to characterize fat. Cardiac MRI and CT imaging are the diagnostic tools of choice for differentiation of fat in soft tissue. MRI demonstrates a well-circumscribed mass with high signal on T1- and T2-weighted sequences, signal

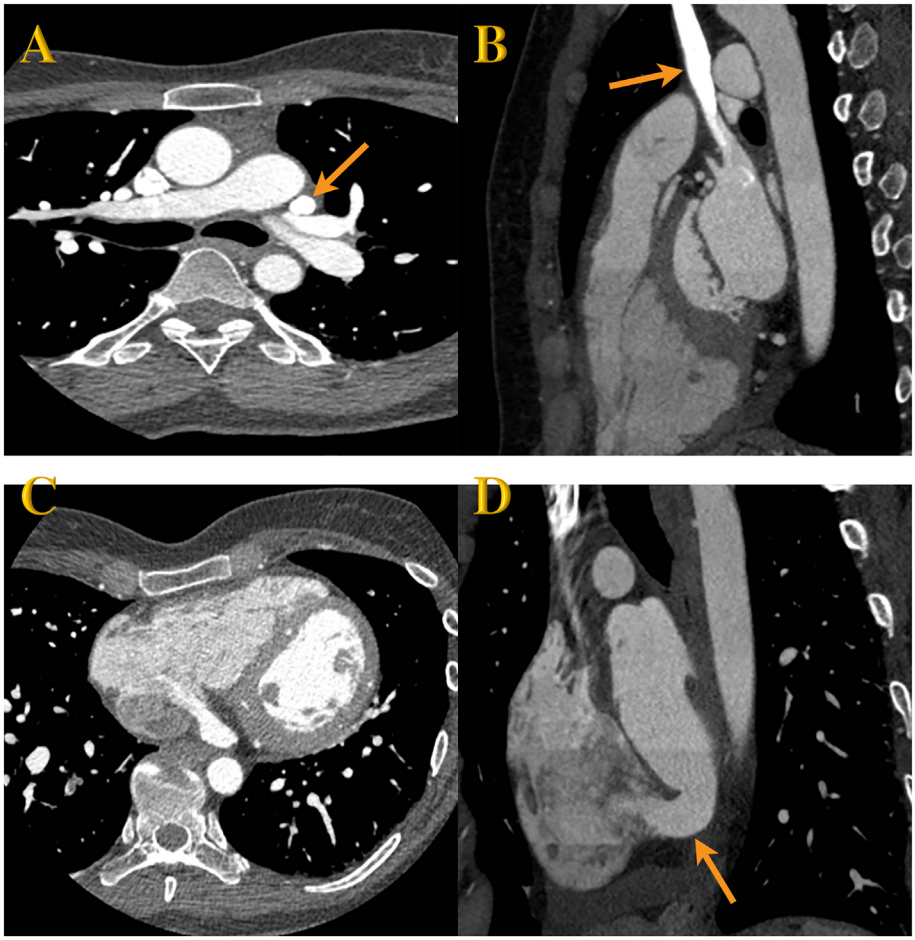

Fig. 6. Persistent left SVC (Image A and B) with right ventricular enlargement (Image C) in a patient with a defect in the wall separating the coronary sinus from the left atrium (Image D) causing a left to right shunt. This defect represents an unroofed coronary sinus. Case courtesy of Dominik Fleischmann, MD, Stanford University Medical Center.

loss on fat suppressed sequences, and lack of enhancement. All of the findings which would be demonstrated buy any macroscopic fat in the body. On CT imaging, the mass demonstrates fat attenuation and does not enhance. Morphologically, an interatrial lipoma involves the fossa ovalis resulting in a more globular appearance and does not have the classic dumbbell-shape (Fig. 8), which is traditionally associated with LHIS [40]. Fig. 8 also demonstrates that interatrial lipomas are not FDG avid on PET.

There is no stablished guideline for management of cardiac lipomas due to its rare occurrence. However, it is accepted that cardiac lipoma in all symptomatic cases need to be resected. Resection should include excision of the capsule to decrease recurrence rate. Close monitoring is an acceptable management for asymptomatic cardiac lipomas with reserving intervention for rapid growing lipomas [41].

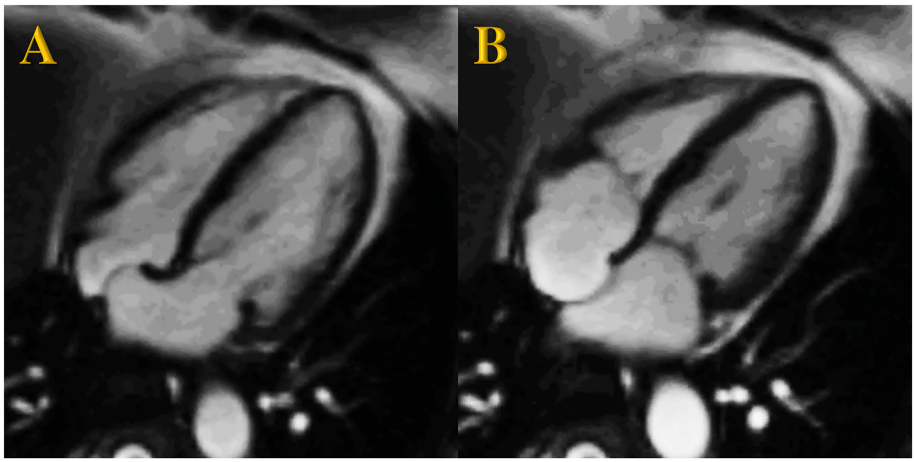

Fig. 7. Four-chamber view with bright blood sequence demonstrates a localized saccular deformity in the atrial septum at the level of fossa ovalis with protrusion to the right and left atrium (excursion measured 19 mm in this patient). Image A in diastole and image B in systole.

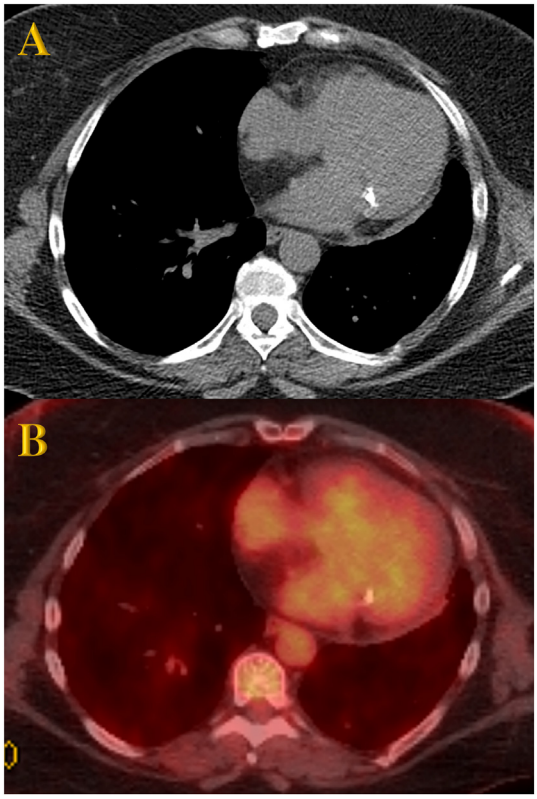

Fig. 8. Axial Non-enhanced CT (image A) at the level of the atria demonstrates a well-defined large mass involving the interatrial septum. The mass demonstrates fat attenuation close to the subcutaneous fat. This mass involves the fossa ovalis, consistent with a lipoma of the interatrial septum. In contrast, lipomatous hypertrophy of the interatrial septum would spare the fossa ovalis taking on a dumbbell shape. Lack of FDG activity on PET/CT (image B) is in favor of interatrial lipoma versus lipomatous hypertrophy of the interatrial septum.

3.2. Lipomatous hypertrophy of the interatrial septum (LHIS)

LHIS is another common adipose-containing benign lesion of the heart that is characterized by accumulation of fat in the interatrial septum. Unlike lipomas, LHIS is not neoplastic or capsulated, and consists of brown fat [1]. Although the etiology of LHIS is not completely understood, one theory is that embryonal mesenchymal cells in the interatrial septum can develop into adipose tissue with the proper stimulus [42]. LHIS is usually seen in older and obese patients with a higher incidence reported in women and those taking steroids. Metabolic disorders such as mediastino-abdominal lipomatosis and long-term parenteral nutrition has been also associated with LHIS. Transthoracic echocardiography studies report an incidence of up to 8%, which is higher than previously expected. This is at least in part related to the increasing age of the general population and advancement in imaging technology [43]. Most cases remain asymptomatic during an individual's lifetime, thus LHIS is usually an incidental finding diagnosed during autopsy or on imaging obtained for an unrelated reason. In less common symptomatic cases, LHIS can cause arrhythmia, obstructive flow symptoms, and rarely death.

A characteristic feature of LHIS seen with all modalities is > 20 mm thickening of the interatrial septum with sparing of the fossa ovalis. CT demonstrates a dumbbell-shaped, fat attenuation, non-enhancing lesion in the interatrial septum with relative sparing of the fossa ovalis [43]. Moderate FDG activity on PET/CT (Fig. 9) is a characteristic imaging feature that differentiates LHIS from an interatrial lipoma. This FDG uptake had been attributed to metabolically active brown fat contained within LHIS. [44,45]. However, there is controversy as the etiology of the FDG uptake in LHIS. Recent reports attributed FDG uptake of LHIS to recurrent inflammation [46]. Cardiac MRI shows interatrial septal thickening with signal characteristics similar to that of subcutaneous fat tissue (high signal in T1- and T2-weighted sequences and low signal in fat suppressed sequences) [47,48].

Asymptomatic cases are best managed with reassurance. Surgical intervention, with resection, and reconstruction of the interatrial septum, is reserved for cases with intractable arrhythmia or severe obstructive disease [43].

3.3. Myxoma

Myxomas are the most common primary benign cardiac tumors. They are mostly solitary and pedunculated with smooth surface and gelatinous consistency [49–51] and are most commonly located at the fossa ovalis in the sub-endocardial tissue of atrial septum [50]. Myxomas are predominantly located in the left atrial cavity (75–80%), up to 15–20% of cases are seen in the right atrium, and 5% arise in the ventricles or are multifocal [49]. This tumor is most commonly seen sporadically in middle-aged (30–60 years old) adults with slightly higher prevalence in women [49,50]. However, myxomas can also occur in familial syndromes (nearly 10% of cases), in which case lesions are often multicentric, in atypical locations, more common in men, and may reoccur even with complete resection [50]. The clinical presentation can vary from asymptomatic to sudden death (rarely) depending on the site, size, and mobility of the tumor as well as the existence of any thrombosis on the surface of the tumor [52]. While patients with right atrial myxomas can be asymptomatic most of the time, they can present acutely with right-sided cardiac dysfunction secondary to tricuspid valve obstruction [49,51]. On the other hand, patients with left atrial myxomas can have more chronic symptoms like dyspnea or orthopnea due to intermittent mitral valve obstruction and pulmonary edema [49]. There are some cases that express the classic triad of the disease: pulmonary edema, progressive heart failure, and embolic events [51].

The first-choice modality to diagnose a cardiac tumor is TTE and, for more a more detailed evaluation, TEE can be done [52]. For confirmation, CT and/or MRI would provide more details of the mass and surrounding tissues and structures, e.g. vasculature, fat, edema, calcification [52]. The definitive diagnosis would be made by biopsy. After diagnosis is confirmed, the best management is surgical treatment [52]. Preoperative differentiation of intraatrial myxoma and thrombus is of high importance due to the vastly different treatment options in the setting of similar clinical symptoms such as peripheral embolization and intracardiac/valvular obstruction [53]. MRI is very helpful in differentiating these two pathologies. Signal characteristics of myxoma are isointense on T1-weighted images, high intensity on T2-weighted images, lack of signal drop on fat suppressed sequences, and heterogeneous enhancement due to areas of necrosis, cystic degeneration, calcification, and hemorrhage (Fig. 10). It is possible for myxoma to have thrombus on its surface [2]. Although, cardiac MRI have significantly improved differentiation of atrial myxoma form clot, several pathologies can still mimic cardiac myxoma including fungal infective endocarditis [54], and primary and secondary cardiac neoplasms [55,56]. Patient's signs and symptoms, lesion location and morphology such as presence or abscess of stack and invasion to the cardiac wall can help differentiate myxoma from other mimics.

Surgical excision of myxoma is safe and effective treatment. Excellent results have been reported from excision of the tumor with or without normal atrial margin. Long term clinical and imaging (echocardiographic) follow up is recommended since rare late recurrence has been reported [57].

3.4. Thrombosis

Intracardiac thrombus is of high clinical significance because of its

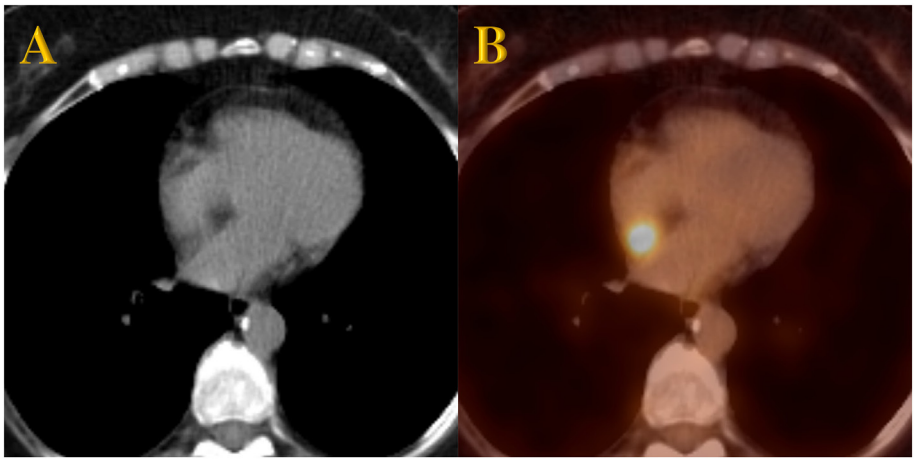

Fig. 9. Axial non-contrast CT demonstrates a dumbbell-shaped fatty infiltration in the interatrial septum with sparing of the fossa ovalis (Image A). PET/CT shows high FDG uptake in the septum confirming brown fat infiltration, consistent with lipomatous hypertrophy of the interatrial septum. (For interpretation of the references to color in this figure legend, the reader is referred to the web version of this article.)

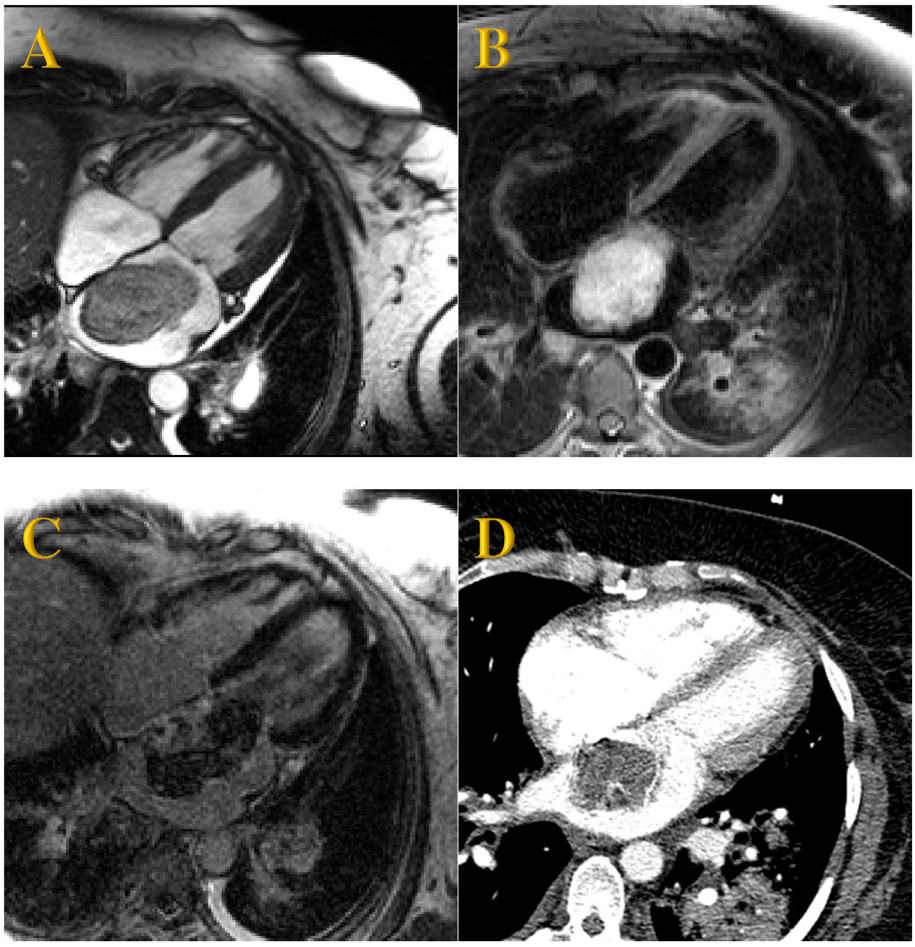

Fig. 10. Mass in the left atrium arises from the interatrial septum adjacent to the fossa ovalis. The mass has heterogeneous signal intensity on bright blood sequence (image A) and heterogeneous high signal intensity on T2-weighted sequence (Image B). Post contrast sequence demonstrates heterogeneous enhancement with foci of enhancement and some area of non-enhancement (image C). Image D demonstrates the CT correlate of this mass on a CT chest angiography. Image findings are consistent with left atrial myxoma.

potential complications, confounded by poor clinical evidence to help clinicians in optimal management. Distinguishing intracardiac thrombi form other filling defect, such as tumors or normal structures (large papillary muscles or trabeculations), is critical since anticoagulation, the treatment for intracardiac thrombi, has serious potential complications. Mitral valve disease/prosthesis, left atrial contractile disorder, such as atrial fibrillation, and left ventricular dysfunction are predisposing factors for left atrial thrombosis. A right atrial thrombosis is less common than a left atrial thrombosis. Right atrial thrombosis usually occurs in patients with central catheters, EKG lines, atrial arrhythmias, or coagulopathy disorders [58]. Heart dysfunction, and tricuspid valve disease are other risk factors for right atrial thrombosis [53]. Both left and right atrial thrombi can cause mechanical valve dysfunction if large enough or become adherent to the mitral or tricuspid valve leaflets. A left atrial thrombus could be a source of peripheral embolism including central nervous system thromboembolic disease. A right atrial

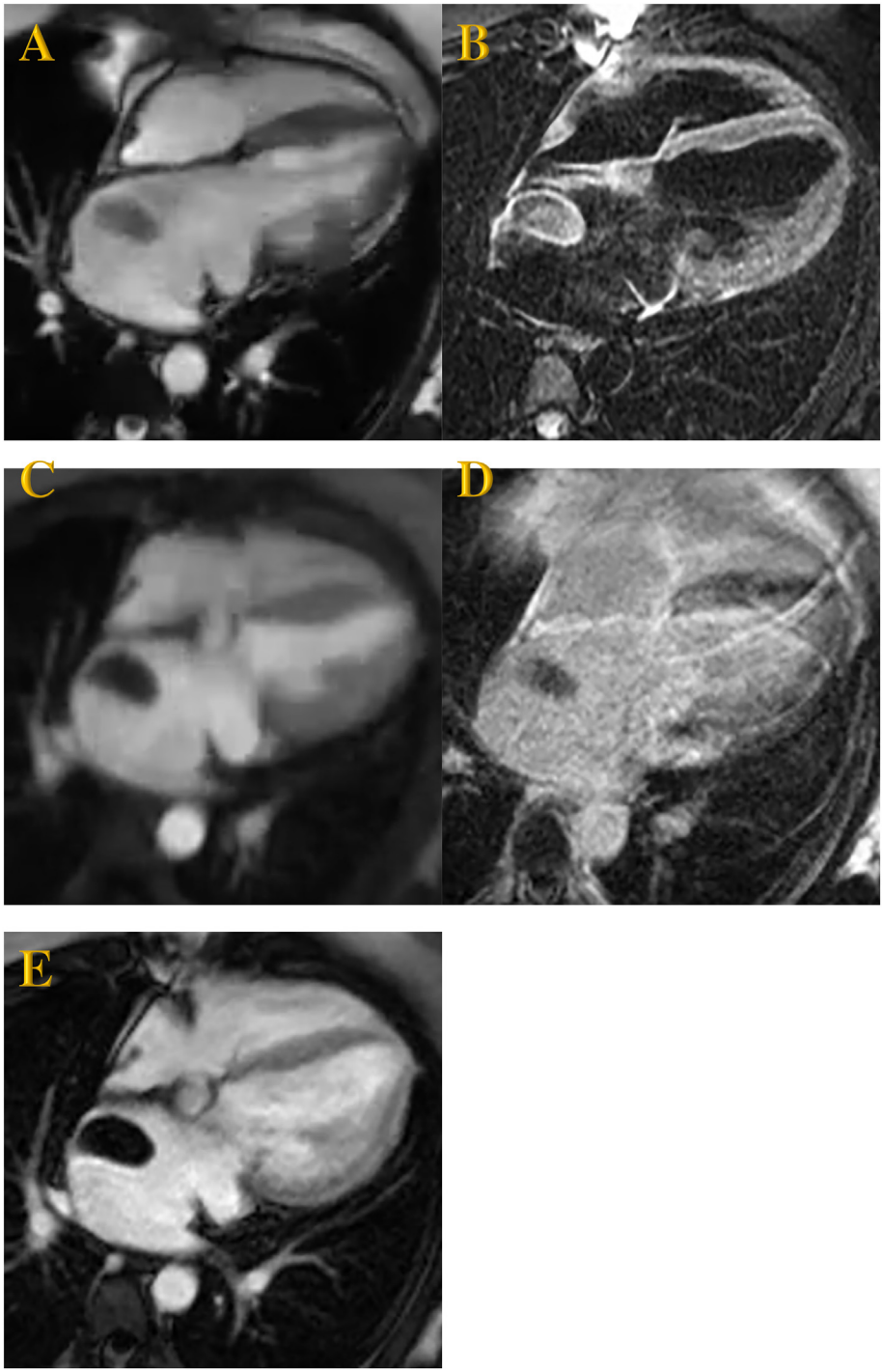

Fig. 11. A 30 × 18 mm large mass appears to be attached/adjacent to the interatrial septum on echocardiography. The mass is isointense on bright blood sequence (image A) and has heterogeneously high signal on T2-weighted sequence (image B). There is poor contrast uptake on first-pass images (image C) and no enhancement on delayed enhance sequence (image D with breathing motion artifact limitation). Dark signal on long TI (600 ms) sequence (image E) confirms lack of enhancing tissue. These findings are consistent with a subacute thrombus.

thrombus can shed emboli to the pulmonary vasculature and cause pulmonary embolism. Although left atrial appendage is the presumed location of thrombus formation in patients with atrial fibrillation, Waller B. et al. reported a 58% rate of thrombosis in the body of the left atrium and 6% thrombosis in the body and appendage in patients with mitral stenosis and left atrial thrombosis [59].

Ventricular thrombi are generally detected by TTE while TEE has a clear advantage for better detection of the bilateral atrial and atrial appendage thrombi via the exam technique which eliminates intervening lung and bone [53]. However, TEE may lead to complications associated with intubation of the esophagus including upper gastroesophageal bleeding and esophageal rupture. TEE is therefore contraindicated in patients with esophageal varices, recent upper gastrointestinal bleeding, and esophageal stricture [60].

Distinguishing large filling defects, specifically myxoma—the most common tumor in the left atrium, from atrial thrombus can be challenging on TEE. To further complicate matters, approximately one third of left atrial myxomas present with thromboembolism of the tumor

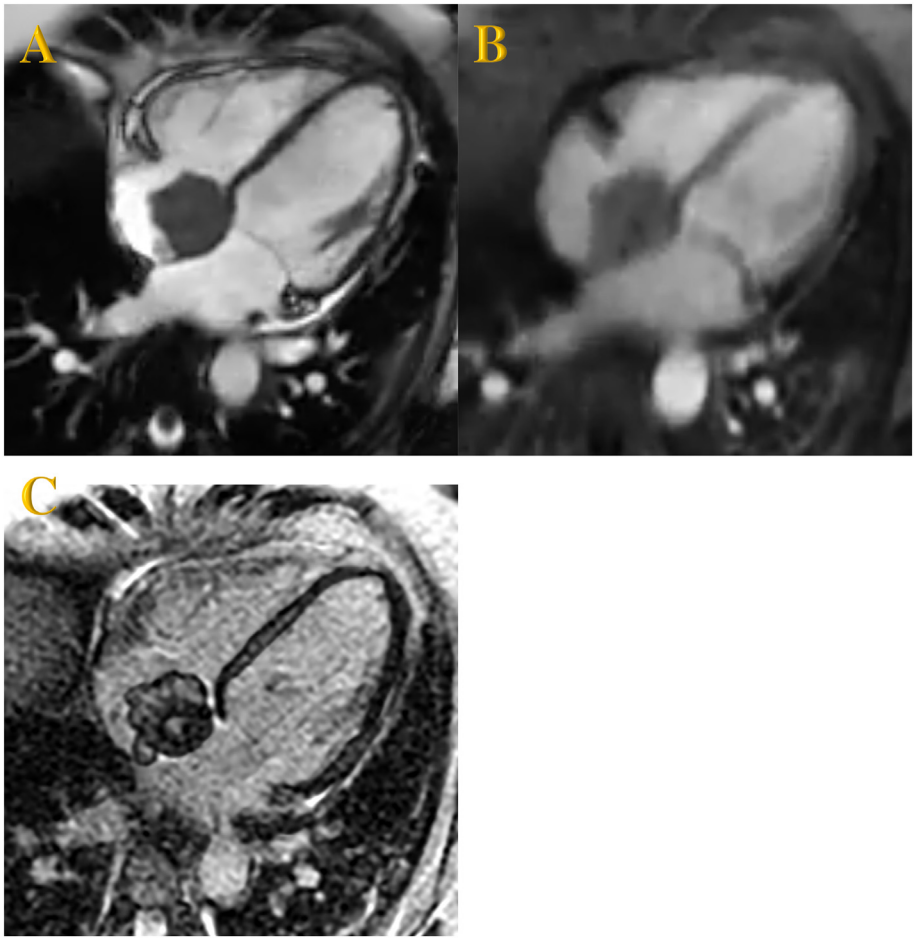

Fig. 12. A 30 × 31 × 40 mm large right atrial mass attached to the interatrial septum is isointense to myocardium on bright blood sequence (image A). There is enhancement similar to the myocardium on perfusion images (image B). The mass also demonstrates heterogeneous enhancement on delayed enhance sequence (image C). These findings are consistent with metastasis in this 57-year-old male with history of lung cancer.

fragments or overlying thrombus, which adds more confusion to the clinical picture of patients with intraatrial filling defects [61]. Like myxoma, an atrial thrombus can be attached to the interatrial septum. Right atrial thrombus adjacent to the base of the interatrial wall can mimic normal variant anatomy like Chiari's network on echocardiography or cross-sectional imaging [62]. Cardiac MRI and use of contrast can significantly help in differentiating intracardiac thrombi from other masses or filling defects including myxoma. T1- and T2-weighted signal characteristics of intraatrial thrombi differ by the age of thrombus. In acute phase, the thrombus shows intermediate T1- and T2-weighted signal intensity due to the presence of oxygenated hemoglobin. A subacute thrombus demonstrates lower T1- and higher T2-weighted signal intensity due to metabolism of hemoglobin to methemoglobin and more internal water content from red blood cell lysis. In the chronic phase, increasing fibrous tissue in the thrombus, resulting in less internal water, leads to low signal intensity on both T1- and T2-weighted images. The other imaging feature that can differentiate thrombus from myxoma is lack of enhancement on first-pass perfusion, or delayed gadolinium enhancement due to lack of blood vessels in thrombus. However, Chronic organized thrombus might have some peripheral enhancement due to its fibrous content [2]. Assessment of enhancement of small lesions is also challenging. Therefore, relying on enhancement to differentiate thrombus from myxoma can be misleading in real life. A much more accurate method for identification of thrombus is the long inversion time (TI: 450–600 ms) sequences. Delayed gadolinium enhanced sequence with long TI, which nulls avascular tissue, is very useful in differentiating intracardiac thrombosis from myxoma and other tumors (Fig. 11). On this sequence, any enhancing tissue (normal myocardium or vascular tumors like myxoma) demonstrate increased intensity while thrombus becomes homogeneously black [63]. T1- and T2-mapping are rapidly expanding techniques with some utility in characterization of cardiac tumors including intracardiac thrombus [64,65]. However, more robust data validating the currently available reports are required [66]. To date, T1- and T2-mapping are still not as accurate as long TI in detection of intracardiac thrombus.

There is lack of robust clinical evidence to guide physicians managing intracardiac thrombus. Despite significant advances in endovascular treatments techniques, anticoagulation is still the main treatment option. Anticoagulation will halt progression and prevent development of new thrombus, but it does not treat the occlusive symptoms that may occur. Therefore, percutaneous or surgical removal of the intracardiac thrombus might be required in certain high risk patients. Precise assessment of risk: benefit with attention to the unique clinical scenario of each case is required before choosing any invasive approach [67].

3.5. Metastatic involvement

Metastatic involvement of the heart is on average 30 times more common than primary cardiac tumors. Approximately 12% of patients with neoplasm are reported to have cardiac metastasis on autopsy [68]. Many cases of cardiac metastasis remain asymptomatic. Clinical presentation depends on the location and size of metastatic deposit which could cause arrhythmia, obstructive or restrictive physiology, or valve

dysfunction. Metastatic involvement of the heart can occur via direct spread from lung or breast cancer, transvenous spread like renal cell carcinoma, hematogenous spread like melanoma and lymphoma, or lymphangitic spread [2]. Although the pericardium is the most common location for cardiac metastasis, metastatic spread of tumor cells can be found in any cardiac location including the interatrial septum.

With the exception of melanoma, which has high T1-weighted signal intensity due to high melanin content, cardiac metastases are usually low in signal on T1-weighted imaging and high in signal on T2-weighted imaging. Post contrast images in either early or late enhancement phase are expected to demonstrate heterogeneous enhancement (Fig. 12) [1].

Surgical management of cardiac metastasis is often challenging due to multifocality if the tumor involvement and involvement of the other organs. Nevertheless, resection is an available option is selected cases with resectable tumor without involvement of other organs [50].

4. Conclusion

With advances in CT and MRI cardiac imaging, radiology plays a significant role in the identification and characterization of interatrial lesions. It is also very important to the medical and surgical management of these lesions. Radiologists and cardiologists must be familiar with the imaging features of interatrial septal lesions so they can appropriately diagnose and guide patient care.

References

[1] O'Donnell DH, Abbara S, Chaithiraphan V, Yared K, Killeen RP, Cury RC, et al. Cardiac tumors: optimal cardiac MR sequences and spectrum of imaging appearances. Am J Roentgenol 2009;193:377–87.
[2] Motwani M, Kidambi A, Herzog BA, Uddin A, Greenwood JP, Plein S. MR imaging of cardiac tumors and masses: a review of methods and clinical applications. Radiology 2013;268(1):26–43.
[3] Hagen PT, Scholz DG, Edwards WD. Incidence and size of patent foramen ovale during the first 10 decades of life: an autopsy study of 965 normal hearts. Mayo Clin Proc 1984;59(1):17–20.
[4] Mohrs OK, Petersen SE, Erkapic D, Rubel C, Schräder R, Nowak B, et al. Diagnosis of patent foramen ovale using contrast-enhanced dynamic MRI: a pilot study. Am J Roentgenol 2005;184(1).
[5] Bogousslavsky J, Garazi S, Jeanrenaud X, Aebischer N, Van Melle G. Stroke recurrence in patients with patent foramen ovale: the Lausanne Study. Lausanne Stroke with Paradoxal Embolism Study Group. Neurology 1996;46(5):1301–5.
[6] Yasunaga D, Hamon M. MDCT of interatrial septum. Diagn Interv Imaging 2015;96(9):891–9.
[7] Nicolay S, Salgado RA, Shivalkar B, Van Herck PL, Vrints C, Parizel PM. CT imaging features of atrioventricular shunts: what the radiologist must know. Insight Imaging 2016;7(1):119–29.
[8] Saremi F, Channual S, Raney A, Gurudevan SV, Narula J, Fowler S, et al. Imaging of patent foramen ovale with 64-section multidetector CT. Radiology 2008;249(2):483–92.
[9] Krishnan SC, Salazar M. Septal pouch in the left atrium: a new anatomical entity with potential for embolic complications. JACC Cardiovasc Interv 2010 Jan 1;3(1):98–104.
[10] Hołda MK, Koziej M, Hołda J, Piątek K, Tyrak K, Chołopiak W, et al. Atrial septal pouch — morphological features and clinical considerations. Int J Cardiol 2016 Oct 1;220:337–42.
[11] Landzberg MJ. Indications for the closure of patent foramen ovale. Heart 2004;90(2):219–24.
[12] Mohr JP, Thompson JLP, Lazar RM, Levin B, Sacco RL, Furie KL, et al. A comparison of warfarin and aspirin for the prevention of recurrent ischemic stroke. N Engl J Med 2001;345:1444–3451.
[13] Santhosh K, Arora R. Cryptogenic stroke: to close a patent foramen ovale or not to close? J Cent Nerv Syst Dis 2018;10:1–9.
[14] Hung J, Landzberg MJ, Jenkins KJ, King MEE, Lock JE, Palacios IF, et al. Closure of patent foramen ovale for paradoxical emboli: intermediate-term risk of recurrent neurological events following transcatheter device placement. J Am Coll Cardiol 2000;35:1311–6.
[15] Dearani JA, Ugurlu BS, Danielson GK, Daly RC, CGA McGregor, Mullany CJ, et al. Surgical patent foramen ovale closure for prevention of paradoxical embolism-related cerebrovascular ischemic events. Circulation 1999;100(19 Suppl):II171-5.
[16] Thomson LEJ, Crowley AL, Heitner JF, Cawley PJ, Weinsaft JW, Kim HW, et al. Direct en face imaging of secundum atrial septal defects by velocity-encoded cardiovascular magnetic resonance in patients evaluated for possible transcatheter closure. Circ Cardiovasc Imaging 2008;1(1):31–40.
[17] Dehghani H, Boyle AJ. Percutaneous device closure of secundum atrial septal defect in older adults. Am J Cardiovasc Dis 2012;2(2):133–42.
[18] Du ZD, Hijazi ZM, Kleinman CS, Silverman NH, Larntz K. Comparison between transcatheter and surgical closure of secundum atrial septal defect in children and adults: results of a multicenter nonrandomized trial. J Am Coll Cardiol 2002;39(11):1836–44.
[19] Berger F, Vogel M, Alexi-Meskishvili V, Lange PE, Lochan R, Worms A, et al. Comparison of results and complications of surgical and amplatzer device closure of atrial septal defects. J Thorac Cardiovasc Surg 1999;118(4):674–80.
[20] Ashley EA, Niebauer J. Cardiology explained. Medicina. London: Remedica; 2004.
[21] Webb G, Gatzoulis MA. Atrial septal defects in the adult: recent progress and overview. Circulation 2006;114(15):1645–53.
[22] Rajiah P, Renapurkar R, Kanne J. Diagnosis of ostium primum defect at multidetector CT in an adult. J Thorac Imaging 2009;24(3):234–6.
[23] Siripornpitak S, Pornkul R, Khowsathit P, Layangool T, Promphan W, Pongpanich B. Cardiac CT angiography in children with congenital heart disease. Eur J Radiol 2013 Jul;82(7):1067–82.
[24] Thangaroopan M, Truong QA, Kalra MK, Yared K, Abbara S. Rare case of an unroofed coronary sinus: diagnosis by multidetector computed tomography. Circulation 2009;119(16).
[25] Bonardi M, Valentini A, Camporotondo R. Unroofed coronary sinus and persistent left superior vena cava: a case report. J Ultrasound 2012;15(3):179–82.
[26] Kong PK, Ahmad F. Unroofed coronary sinus and persistent left superior vena cava. Eur J Echocardiogr 2007;8:398–401.
[27] Kwak JG, Lee C, Choi EY, Song JY, Lee CH. Dilated unroofed coronary sinus mimicking cor triatriatum in cardiac-type total anomalous pulmonary venous connection. J Card Surg 2012;27(5):621–3.
[28] Pérez Matos AJ, Planken RN, Bouma BJ, Groenink M, Backx APCM, de Winter RJ, et al. Unroofed coronary sinus newly diagnosed in adult patients after corrected congenital heart disease. Neth Hear J 2014;22(5):240–5.
[29] Cabanes L, Mas JL, Cohen A, Amarenco P, Cabanes P a, Oubary P, et al. Atrial septal aneurysm and patent foramen ovale as risk factors for cryptogenic stroke in patients less than 55 years of age. A study using transesophageal echocardiography. Stroke 1993;24(12):1865–73.
[30] Oyedeji AT, Okunola O, Sani MU. Atrial septal aneurysm mimicking a cor triatriatum sinister: a case report and review of the literature. Clin Med Insight Case Rep 2012;5:143–7.
[31] Ewert P, Berger F, Vogel M, Dähnert I, Alexi-Meshkishvili V, Lange PE. Morphology of perforated atrial septal aneurysm suitable for closure by transcatheter device placement. Heart 2000;84:327–31.
[32] Morelli S, Voci P, Morabito G, Sgreccia A, De Marzio P, Marzano F, et al. Atrial septal aneurysm and cardiac arrhythmias. Int J Cardiol 1995;49(3):257–65.
[33] Belkin RN, Kisslo J. Atrial septal aneurysm: recognition and clinical relevance. Am Heart J 1990;120(4):948–57.
[34] Hanley PC, Tajik AJ, Hynes JK, Edwards WD, Reeder GS, Hagler DJ, et al. Diagnosis and classification of atrial septal aneurysm by two-dimensional echocardiography: report of 80 consecutive cases. J Am Coll Cardiol 1985;6(6):1370–82.
[35] Pearson AC, Nagelhout D, Castello R, Gomez CR, Labovitz AJ. Atrial septal aneurysm and stroke: a transesophageal echocardiographic study. J Am Coll Cardiol 1991;18:1223–9.
[36] Galrinho A, Branco LM, De Sousa L, Pinto F, Ferreira R. Giant interatrial septal aneurysms mimicking quistic masses: two cases with different therapeutic options. Rev Port Cardiol 2010;29(9):1429–32.
[37] Burger AJ, Sherman HB, Charlamb MJ. Low incidence of embolic strokes with atrial septal aneurysms: a prospective, long-term study. Am Heart J 2000;139(1):149–52.
[38] Kassop D, Donovan MS, Cheezum MK, Nguyen BT, Gambill NB, Blankstein R, et al. Cardiac masses on cardiac CT: a review. Curr Cardiovasc Imaging Rep 2014;7(8):1–13.
[39] Laura DM, Donnino R, Kim EE, Benenstein R, Freedberg RS, Saric M. Lipomatous atrial septal hypertrophy: a review of its anatomy, pathophysiology, multimodality imaging, and relevance to percutaneous interventions. J Am Soc Echocardiogr 2016;29(8):717–23.
[40] Rojas CA, Jaimes CE, El-Sherief AH, Medina HM, Chung JH, Ghoshhajra B, et al. Cardiac CT of non-shunt pathology of the interatrial septum. J Cardiovasc Comput Tomogr 2011;5(2):93.
[41] Naseerullah FS, Javaiya H, Murthy A. Cardiac lipoma: an uncharacteristically large intra-atrial mass causing symptoms. Case Rep Cardiol 2018;6(2018):3531982.
[42] Meaney JFM, Kazerooni EA, Jamadar DA, Korobkin M. CT appearance of lipomatous hypertrophy of the interatrial septum. Am J Roentgenol 1997;168(4):1081–4.
[43] Xanthos T, Giannakopoulos N, Papadimitriou L. Lipomatous hypertrophy of the interatrial septum: a pathological and clinical approach. Int J Cardiol 2007;121:4–8.
[44] Shinto A, Kamaleshwaran K, Sudhakar N, Shibu D, Kurup ERR. Persistent high grade flurodeoxyglucose uptake in lipomatous hypertrophy of the interatrial septum on dual time point imaging and with ambient warming. World J Nucl Med 2014;13(1):62.
[45] Klein MA, Scalcione LR, Youn T, Shah RA, Katz DS, Sung WW, et al. Intensely hypermetabolic lipomatous hypertrophy of the interatrial septum on 18-FDG PET with MRI and CT correlation. Clin Nucl Med 2010;35(12):972–3.
[46] Zukotynski KA, Israel DA, Kim CK. FDG uptake in lipomatous hypertrophy of the interatrial septum is not likely related to brown adipose tissue. Clin Nucl Med 2011 Sep;36(9):767–9.
[47] Bajaj RR, Deva D, Kirpalani A, Yan RT, Chow CM, Lo V, et al. Cardiac magnetic resonance imaging for non-invasive diagnosis of lipomatous hypertrophy of interatrial septum. Indian Heart J 2014;66(2):244–6.
[48] Tatli S, O'Gara PT, Lambert J, Kwong R, Byrne JG, Yucel EK. MRI of atypical lipomatous hypertrophy of the interatrial septum. Am J Roentgenol 2004;182(3):598–600.

[49] Abbas A, Garfath-Cox KAG, Brown IW, Shambrook JS, Peebles CR, Harden SP. Cardiac MR assessment of cardiac myxomas. Br J Radiol 2015;88(1045).
[50] Hoffmeier A, Sindermann JR, Scheld HH, Martens S. Cardiac tumors–diagnosis and surgical treatment. Dtsch Arztebl Int 2014;111(12):205–11.
[51] Kayançiçek H, Khalil E, Keskin G, Alataş Ö, Hafız E, Faruk Doğan Ö. Ten years' clinical experience of cardiac myxoma: diagnosis, treatment, and clinical outcomes. Anatol J Cardiol 2018;19(2):157–8.
[52] Roever L, Casella-Filho A, Dourado PMM, Resende ES, Chagas ACP. Cardiac tumors: a brief commentary. Front Public Health 2014;2:264.
[53] Turhan S, Ozcan OU, Erol C. Imaging of intracardiac thrombus. vol. 55. Cor et Vasa; 2013.
[54] Pasternak R, Cannom D, Cohen L. Echocardiographic diagnosis of large fungal verruca attached to mitral valve. Br Heart J 1976;38(11):1209–12.
[55] Mazzola A, Spano JP, Valente M, Gregorini R, Villani C, Di Eusanio M, et al. Leiomyosarcoma of the left atrium mimicking a left atrial myxoma. J Thorac Cardiovasc Surg 2006;131(1):224–6.
[56] Quigley MM. A unique atrial primary cardiac lymphoma mimicking myxoma presenting with embolic stroke: a case report. Blood 2003;101:4708–10.
[57] Lone R a, Ahanger a G, Singh S, Mehmood W, Shah S, Lone G, et al. Atrial myxoma: trends in management. Int J Health Sci 2008;2(2):141–51.
[58] Malik SB, Kwan D, Shah AB, Hsu JY. The right atrium: gateway to the heart—-anatomic and pathologic imaging findings. Radiographics 2015;35(1):14–31.
[59] Waller BF, Grider L, Rohr TM, Mclaughlin T, Taliercio CP, Fetters J. Intracardiac thrombi: frequency, location, etiology, and complications: a morphologic review—part IV. Clin Cardiol 1995;18(11):669–74.
[60] Hilberath JN, Oakes DA, Shernan SK, Bulwer BE, D'Ambra MN, Eltzschig HK. Safety of transesophageal echocardiography. J Am Soc Echocardiogr 2010;23:1115–27.
[61] Pinede L, Duhaut P, Loire R. Clinical presentation of left atrial cardiac myxoma: a series of 112 consecutive cases. Medicine (Baltimore) 2001;80(3):159–72.
[62] Lacobellis A, Puletti M, Vitarelli A. Images in cardiology: worm-shaped thrombus mimicking Chiari's network in a cocaine user. Heart 2002;88(1):4.
[63] Weinsaft JW, Kim HW, Shah DJ, Klem I, Crowley AL, Brosnan R, et al. Detection of left ventricular thrombus by delayed-enhancement cardiovascular magnetic resonance. Prevalence and markers in patients with systolic dysfunction. J Am Coll Cardiol 2008;52(2):148–57.
[64] Caspar T, El Ghannudi S, Ohana M, Labani A, Lawson A, Ohlmann P, et al. Magnetic resonance evaluation of cardiac thrombi and masses by T1 and T2 mapping: an observational study. Int J Card Imaging 2017;33(4):551–9.
[65] Pazos-López P, Pozo E, Siqueira ME, García-Lunar I, Cham M, Jacobi A, et al. Value of CMR for the differential diagnosis of cardiac masses. JACC Cardiovasc Imaging 2014;7(9):896–905.
[66] Desai MY, Jellis CL. Differentiation of cardiac masses by CMR: judging a character by the company it keeps. JACC Cardiovasc Imaging 2014;7(9):906–8.
[67] Egolum UO, Stover DG, Anthony R, Wasserman AM, Lenihan D, Damp JB. Intracardiac thrombus: diagnosis, complications and management. Am J Med Sci 2013;345(5):391–5.
[68] Abraham KP, Reddy V, Gattuso P. Neoplasms metastatic to the heart: review of 3314 consecutive autopsies. Am J Cardiovasc Pathol 1990;3(3):195–8.